U.S. DEPARTMENT OF ENERGY | Office of Science

DOE/SC-ARM-15-008

Lidar Inter-Comparison Exercise Final Campaign Report

A Protat
S Young

February 2015

ARM
CLIMATE RESEARCH FACILITY

DISCLAIMER

DOE/SC-ARM-15-008

Lidar Inter-Comparison Exercise Final Campaign Report

A Protat
S Young

February 2015

Work supported by the U.S. Department of Energy,
Office of Science, Office of Biological and Environmental Research

Executive Summary

The objective of this field campaign was to evaluate the performance of the new Leosphere R-MAN 510 lidar, procured by the Australian Bureau of Meteorology, by testing it against the MicroPulse Lidar (MPL) and Raman lidars, at the Darwin Atmospheric Radiation Measurement (ARM) site. This lidar is an eye-safe (355 nm), turn-key mini Raman lidar, which allows for the detection of aerosols and cloud properties, and the retrieval of particulate extinction profiles. To accomplish this evaluation, the R-MAN 510 lidar has been operated at the Darwin ARM site, next to the MPL, Raman lidar, and Vaisala ceilometer (VCEIL) for three months (from 20 January 2013 to 20 April 2013) in order to collect a sufficient sample size for statistical comparisons.

Comparisons with the Raman lidar were unable to be conducted, since the Raman lidar attenuated backscatter and depolarization ratio product were not available. However, a new product has been delivered to the ARM Data Archive as a value-added product, hence the study will continue.

Despite the unavailability of data from the Raman lidar, software has been developed to analyze the different space and time resolutions of the other lidars and project that data onto a common grid, thus permitting detailed comparison of the instruments' performance as well as enhanced analysis of clouds and aerosols through the use of composite data products, such as the ratios of attenuated backscatters, attenuated scattering ratios and depolarization ratios. Comparisons between the MPL and R-MAN510 lidar data exhibit large differences in total attenuated backscatter at 355 and 532 nm, attenuated scattering ratios, and aerosol volume depolarization ratios. Differences in attenuated backscatter result mainly from the different relative contributions of scattering from molecules and particles at different wavelengths, but there are some additional differences that will require further investigation. The differences in volume depolarization ratios are due to the much larger contribution of molecular returns to the volume depolarization ratio (five times larger at 355 nm than at 532 nm). The R-MAN510 lidar is also found to be much less sensitive to daylight solar background illumination, which is greater at the visible wavelength compared to ultraviolet (UV) wavelengths.

Acronyms and Abbreviations

MPL	MicroPulse Lidar
ABCR	Centre for Australian Weather and Climate Research
ARCS	Atmospheric Radiation and Cloud Station
ARM	Atmospheric Radiation Measurement
CAWCR	Centre for Australian Weather and Climate Research
UV	Ultraviolet
VCEIL	Vaisala Ceilometer
UTC	Coordinated Universal Time
PBL	Planetary Boundary Layer

Contents

Figures

1.0 Background

The objective of this field campaign is to evaluate the performance of the new Leosphere R-MAN 510 lidar, procured by the Australian Bureau of Meteorology, by testing it against the MPL and Raman lidars, at the Darwin ARM site. This lidar is an eye-safe (355 nm), turn-key mini Raman lidar, which allows for the detection of aerosols and cloud properties, and the retrieval of visible extinction. To achieve this objective, the R-MAN 510 lidar was installed at the Darwin ARM site, next to the MPL and Raman lidar, for an operation period of three months (from 21 January 2013 to 30 April 2013), in order to collect a sufficient sample size for statistical comparisons. The data collected also examined the nature of the aerosol throughout the Darwin site. Thorough comparison of the instruments' performances requires comparative statistical analyses of the instruments' abilities to detect various cloud and aerosol layers and retrieve their particulate backscatter or extinction profiles. Although some data products on cloud base and top heights are available for the MPL data, there is no extinction data product available, since automated algorithms capable of retrieving such data in realistic complex atmospheres are difficult to implement reliably. Therefore, the assessments are based on comparison of the various directly measured parameters, which were combined after mapping the data from each instrument to a common height versus time grid.

2.0 Notable Events or Highlights

Total attenuated backscatters at 355 nm and 532 nm differ in ice clouds as a consequence of the different relative contributions of molecular and particulate scattering at the different wavelengths (e.g. Molecular scattering is five times greater at 355 nm than at 532 nm and forty three times greater at 910 nm). Thus, the total backscatter signal increases at shorter wavelengths, but the stronger scattering results in greater attenuation with range, which causes the molecular contribution to the total signal at shorter wavelengths to decrease more rapidly, than at longer wavelengths. Other complicating factors are attenuation due to water vapor at 910 nm and greater attenuation due to ozone at 532 nm. The attenuated scattering ratio was found to be a more useful parameter; which is the ratio of the calibrated, measured signal to that of the modelled signal expected from a purely molecular atmosphere. Some unexplained differences were noted, particularly in some water cloud layers, which will require further study. Volume depolarization ratios, including particulate and molecular returns, also differ noticeably, due to the larger contribution of molecular returns at 355nm. Overall, the R-MAN510 355 nm lidar is less sensitive to daylight solar background illumination, which is greater at the visible wavelength than in UV wavelengths, resulting in better detection capabilities of the R-MAN510 lidar relative to the MPL. The most notable result was the capability of distinguishing between smoke and dust layers using the composite data products developed (Young et al. 2014).

3.0 Lessons Learned

Identifying instances with air clean enough for proper calibration of the lidars proved very difficult, particularly at a tropical coastal site, during the wet season. Thus, a period of three months for inter-comparison of instrument performance was too short a duration to easily identify a reasonable number of occurrences of clear, suitable conditions conducive to precise lidar calibration measurements. However, throughout the duration of the study, a sufficient number of cases were identified to enable reasonable

calibrations, albeit with significant uncertainties in MPL data. It is recommended that future studies be conducted over a longer period of time.

4.0 Results

The main ARM instruments included in this study were the latest MicroPulse Lidar (MPL), which measures two polarization components of the backscattered 532 nm radiation by switching quickly between the two receiver configurations, the Vaisala CL31 ceilometer, which operates at 910 nm, and the CAWCR Leosphere R-MAN510 lidar, which operates at 355 nm and operated at the Darwin ARCS between late January 2013 and the end of April 2013.

4.1 Preliminary Tasks

Preliminary work on lidar data was described in a previous ARM report (Young et al. 2014), therefore, only a brief summary will be provided here. Data reading software has been developed to create files where lidar data is mapped onto a common height-time grid using interpolation or averaging. This allows for direct comparison of the different lidar geophysical parameters of interest: attenuated backscatter, attenuated scattering ratio, depolarization ratio, and ratios of differences in these parameters for the different lidar pairs. Visualization software developed to plot lidar parameters uses the same color scale, allowing for direct quantitative comparisons. The ARM NetCDF radiosonde files were used during analysis to calculate the vertical profiles of molecular scattering, transmittance, and water vapor absorption.

More work was needed for the Leosphere R-MAN-510 lidar. The overlap function of the instrument, which accounts for any incomplete overlap between the transmitter beam and the cone defined by the receiver's field of view, (whose optical axis is displaced laterally from that of the laser transmitter), was not provided by the manufacturer and had to be determined. For the R-MAN510, the overlap function reaches unity (i.e., full overlap is achieved) at about 500 m range from the lidar. All data retrieved from closer ranges requires correction using the overlap function. Therefore, the data set was carefully searched to find suitable periods for measuring this overlap function. The detailed procedure is described in Young et al. (2014). Lidar calibration was achieved by fitting the measured signal, in a region of low aerosol content, to a modelled atmospheric backscatter signal. The model atmosphere was calculated from radiosonde pressure and temperature profiles (Young et al. 2014).

Despite additional complications described in Young et al. (2014), the fast-switching MPL data have also been calibrated using the same procedure, yielding satisfactory results.

4.2 Main Results

Data was collected between January.21 and April.30, 2013, during which time a high number of lidars were present at the Darwin ARM site. Four days have been selected from this period to perform detailed comparative analyses on the data retrieved, based on the favorable conditions present during those days (lidars in excellent operational conditions, no complex meteorological situations, well-identified aerosol and cirrus layers).

The first case was sampled on the April 18, 2013. Vaisala Ceilometer and MPL attenuated backscatter, linear depolarization ratio, and the ratio of 910 to 532 attenuated backscatters, (usually referred to as the attenuated backscatter color ratio or ABCR), are plotted in Figure. 1.

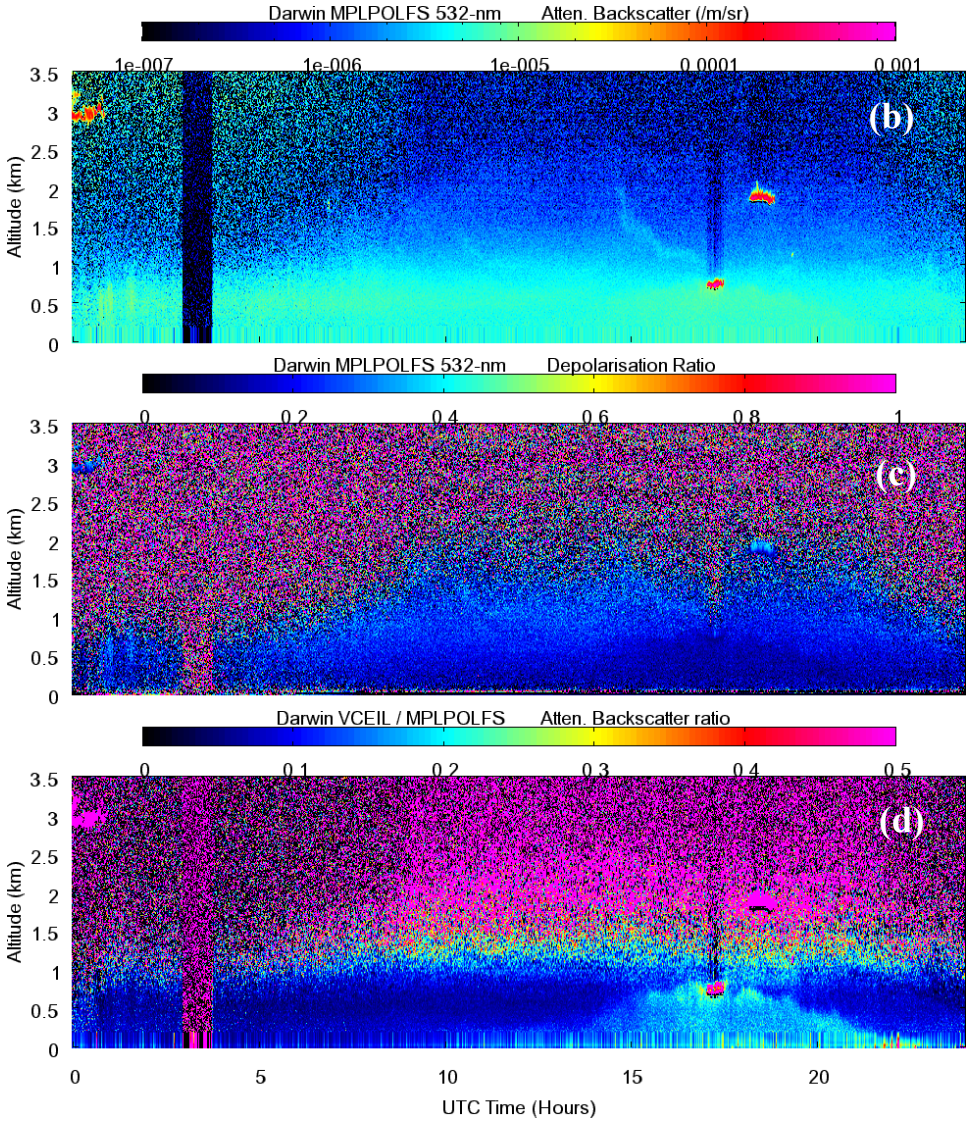

Figure 1. April 18, 2013. Height versus time plots of (a) Vaisala CL31 910 nm Attenuated Backscatter (m.sr)-1 , (b) MPL 532 nm Attenuated Backscatter (m.sr)-1, (c) Micropulse Lidar 532 nm Depolarization Ratio, and (d) Ratio of (a) / (b).

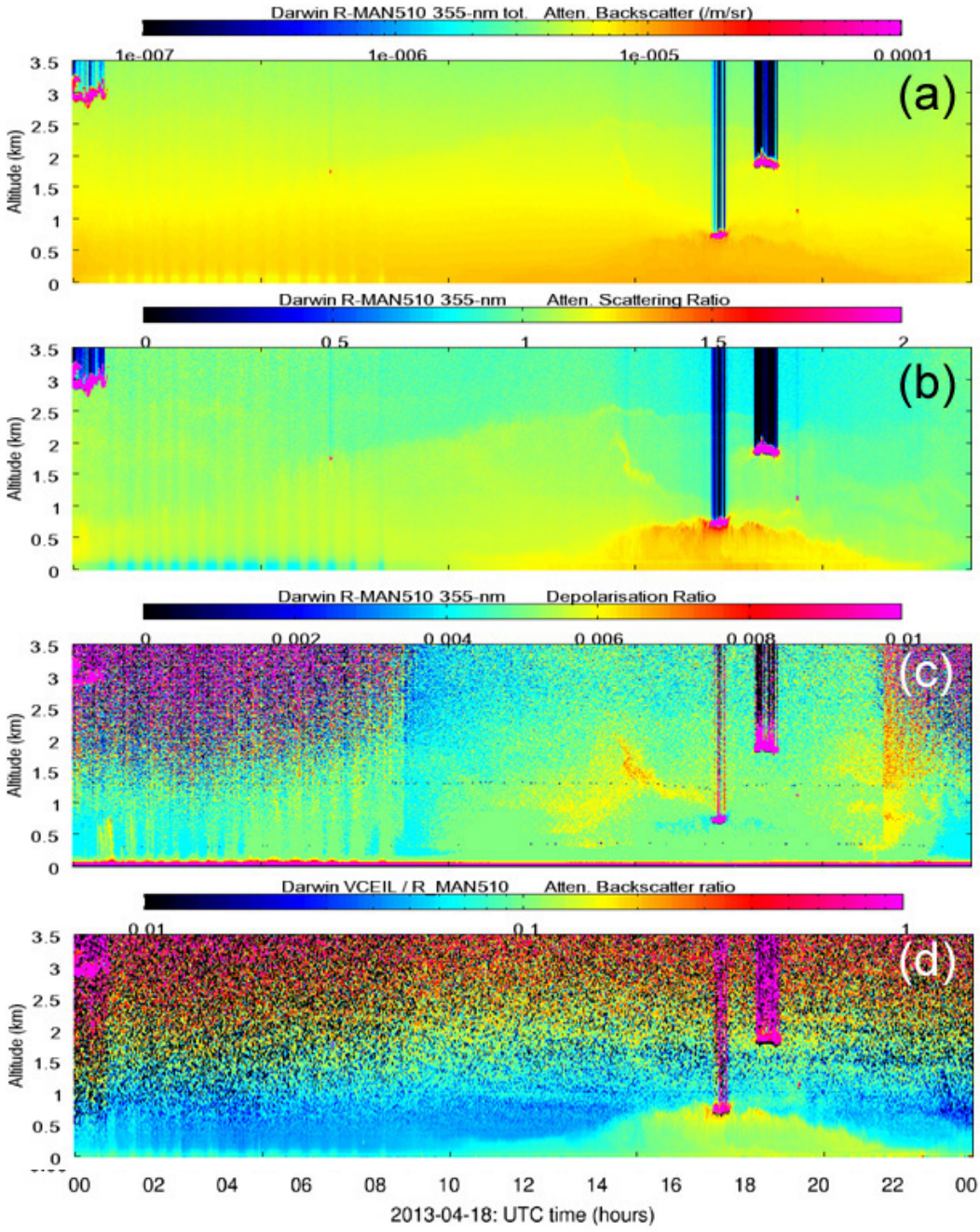

Figure 2. 18 April 2013. Height versus time plots of R-MAN510 355 nm (a) Attenuated Backscatter (m.sr)-1, (b) Attenuated Scattering Ratio (c) linear depolarization ratio, (d) Ratio of Attenuated Backscatter at 910 / 355 nm.

Data from the Leosphere R-MAN510 is plotted in Figure 2. Panel 2(a) is the 355 nm attenuated backscatter, (b) is the attenuated scattering ratio (ratio of measured attenuated backscatter to the modelled molecular backscatter), (c) is the depolarization ratio (smaller at 355 nm than at 532 nm because of the weaker contribution of aerosol backscatter to the total signal) and (d) is the 910 nm to 355 nm ABCR calculated from the ceilometer and R-MAN 510 data.

In these plots, a clearly-defined nocturnal layer is found whose depth increases from zero at around 1400 UTC, grows to 750 m., and then drops to zero again by about 2230 UTC. When the nocturnal layer reaches its maximum height, it is topped by a water cloud, as shown by the strong attenuated backscatter, low depolarization ratio, and strong signal extinction above the water cloud base. The aerosol layer is characterized by a very low depolarization ratio at both 532 nm and 355 nm, indicative of spherical particles. The enhanced ABCR values suggest that these particles are larger than in other regions.

The nocturnal layer grows inside a much deeper aerosol layer, reaching a maximum altitude of about 2.5 km around 1500 UTC, after which time the depth of the layer decreases rapidly and remains below 1000 m for the rest of the day. This layer can be distinguished from the nocturnal layer, as it is characterized by an enhanced depolarization ratio of 355 nm. (This layer is most visible in the 355 nm attenuated scattering ratio plot). Due to the tenuous nature of the layer, the 910 nm to 532 nm ABCR values for the layer are mostly hidden in the noise.

Comparisons of attenuated backscatter, attenuated scattering ratio, and volume depolarization ratio in clouds were also conducted using data collected on January 28, 2013, as this day shows a range of interesting features, including high cirrus, mid-level, and low-level clouds and precipitation, as well as different types of aerosols in the planetary boundary layer and free troposphere. Attenuated backscatters from the R-MAN510, MPL, and VCEIL are shown in Figure 3. Results from the ratio displayed in Figure 3 (d) indicate that the MPL attenuated backscatters are much larger, by a factor of 2 to 3, than those measured by the R-MAN510 within the high cirrus. This difference results mostly from greater attenuation with range at the shorter wavelength, as a consequence of the more prevalent molecular scattering. Therefore, when the cloud base is reached around 12.5 km, the 355-nm attenuated backscatter is lower than the 532-nm signal. The ceilometer attenuated backscatters in the lower atmosphere are found to be lower than the R-MAN510 values. The reason for these differences can be attributed to the attenuated backscatter signal containing both particulate and molecular contributions, and the R-MAN510's molecular signal at 355 nm, being forty-three times larger than that measured by the ceilometer at 910 nm. Also, the greater rate of molecular attenuation at 355 nm is not as significant over the shorter range as it is in the cirrus layer. The data indicate that the MPL's signal is more strongly affected by the daytime solar background illumination, which is greater at the visible wavelength than in the UV wavelengths, or at 910 nm. Consequently, the MPL's receiver should be blocked around local noon, whereas the R-MAN510 and the ceilometer do not require this action.

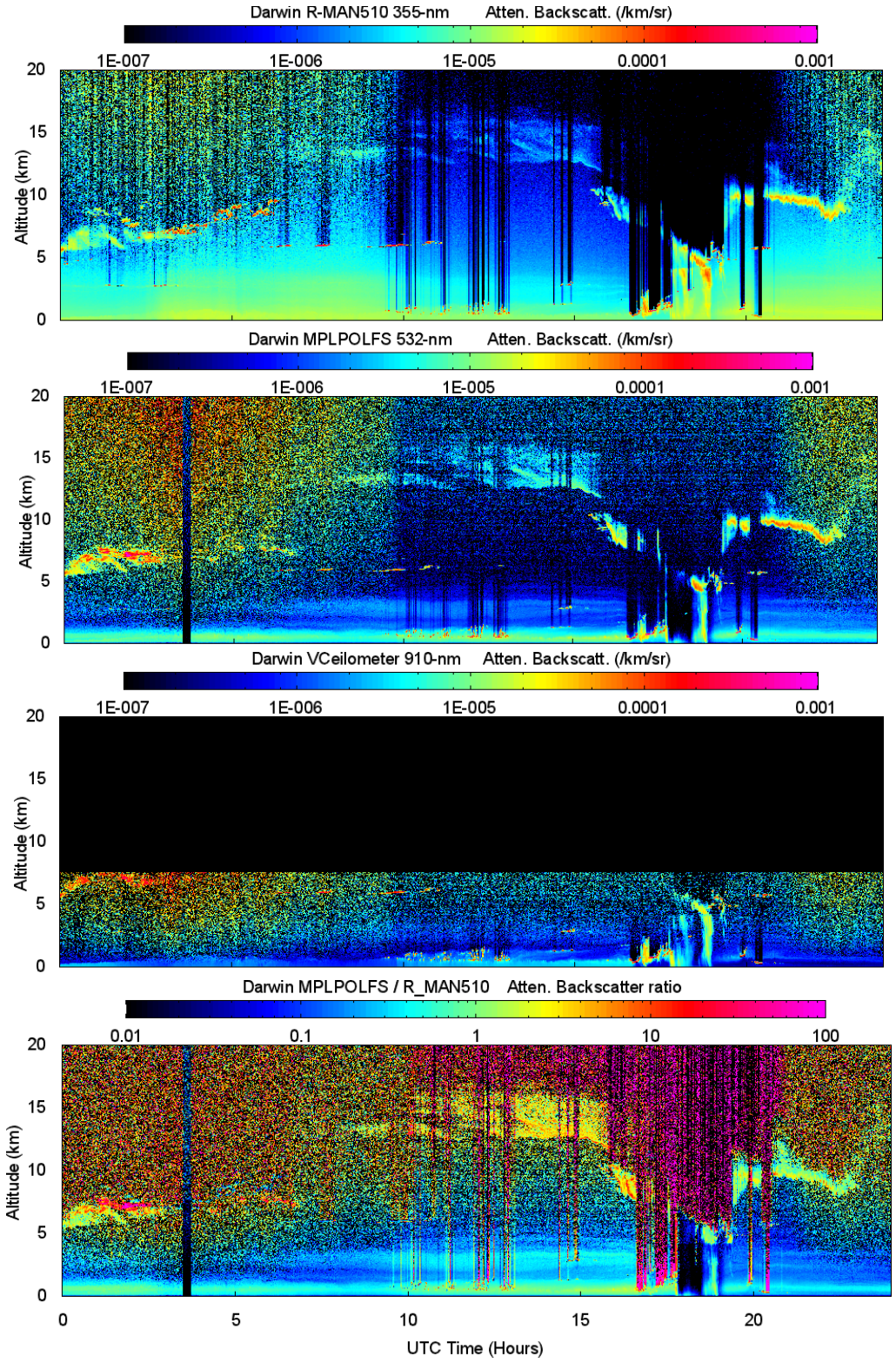

Figure 3. 28 January 2013. From top to bottom of plot: Total attenuated backscatter from the R-MAN510, MPL, and the Vaisala Ceilometer, and the MPL / R-MAN510 ratio of total attenuated backscatter.

Scattering ratios, alternatively, are not affected by differential rates of molecular attenuation at the two wavelengths. Figure 4 illustrates the ratios of attenuated scattering from the two lidars, which appear even larger than the ratios of attenuated backscatter (Figure 3(d)). The MPL attenuated scattering ratios appear approximately 5-7 times higher than those from the R-MAN510. Although the different rate of molecular attenuation is cancelled in the scattering ratio plots, the difference results from the greater contribution (five times) of the molecular component to the total signal, which leads to a lower scattering (i.e. total to molecular) ratio at the shorter wavelength.

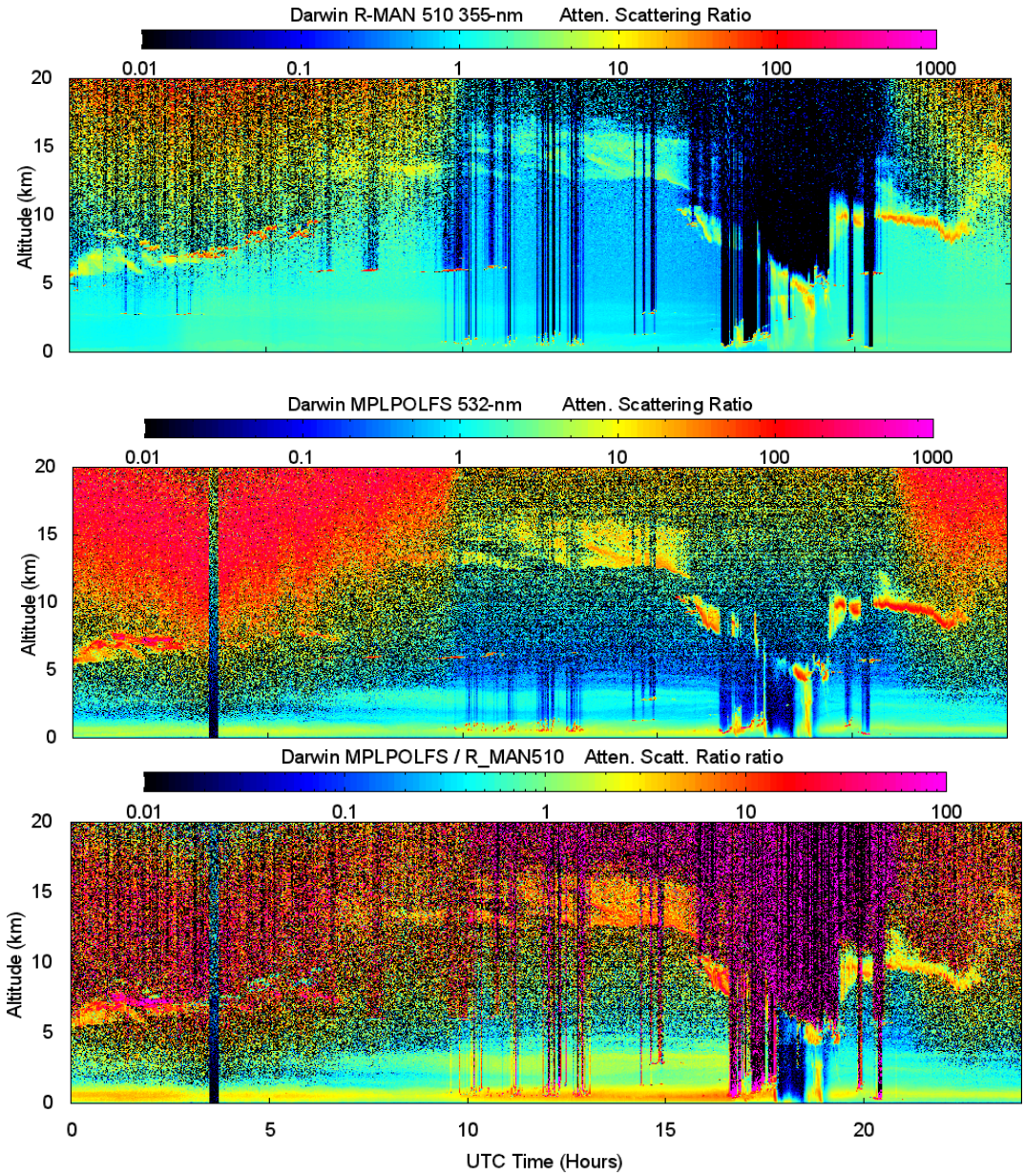

Figure 4. Attenuated scattering ratio from the R-MAN510 (top), and MPL (middle) and the MPL / R-MAN510 ratio of attenuated scattering ratio (bottom).

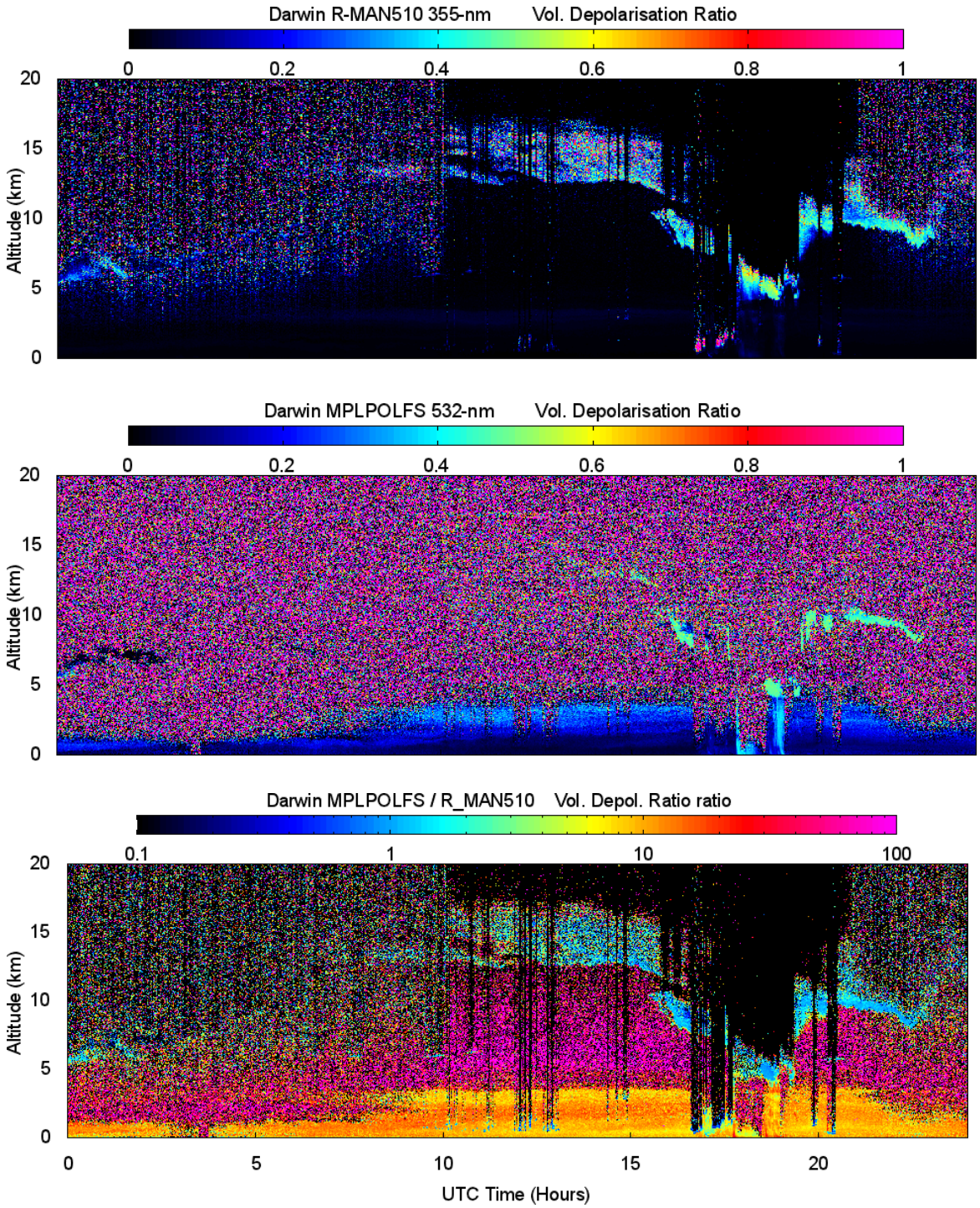

Figure 5. January 28, 2013. Volume depolarization ratio from the R-MAN510 (top), from the MPL (middle) and the ratio of the two (bottom). The volume depolarization ratio includes both particulate and molecular contributions.

Comparisons of volume depolarization ratios (including both particulate and molecular returns) are shown in Figure 5. (Note: The MPL depolarizations have been corrected using the technique outlined in Flynn et al. (2007)). Figure 5 illustrates that depolarization ratios in ice clouds are in reasonably good agreement.

Similarly to the attenuated backscatter, the MPL seems more strongly affected by the daytime solar background illumination, resulting in a lower detection capability than the R-MAN510.

The PBL aerosol has depolarization ratios close to zero (as observed by both lidars), indicating spherical particles (presumably a maritime aerosol), whereas the very weak layer above the PBL contains measurable depolarization ratios, possibly indicative of dust. The R-MAN volume depolarization ratios in the aerosol layers are much lower than the MPL values. As the R-MAN510, operating at 355 nm, has five times the molecular contribution (about 3 to 4% depolarization) than the 532-nm MPL signal, its total measured volume depolarization is, as expected, smaller than that for the MPL.

5.0 References

Flynn CJ, A Mendoza, Y Zheng, and S Mathur. 2007. "Novel Polarization-Sensitive Micropulse Lidar Measurement Technique." *Optics Express* 15: 2785–2790.

Stuart Y, Y Qin, R Mitchell, and S Campbell. 2014. "Radiative Forcing by Australian Tropical Aerosol: Understanding the Role of Dust."

www.arm.gov

U.S. DEPARTMENT OF
ENERGY

Office of Science